https://dx.doi.org/10.1016/j.conbuildmat.2023.133239

Words: 7734

Performance of Oil-Absorbing Organogel Polystyrene-Stearyl Methacrylate as A Fume Suppressant of Asphalt Binder

Meizhao Han[1, 2], Yiqiu Tan[1, 3], Zhen Leng[2]*, Fuliao Zou[2], Shuai Li[1], Jilu Li[1], Chao Zhang[1]*

1. School of Transportation Science and Engineering, Harbin Institute of Technology, Harbin 150090, Heilongjiang, China

2. Department of Civil and Environmental Engineering, The Hong Kong Polytechnic University, Hong Kong, China

3. State Key Laboratory of Urban Water Resource and Environment, Harbin Institute of Technology, Harbin 150090, Heilongjiang, China

Abstract

Hazardous fumes can be generated during the high-temperature construction of asphalt pavement. Various fume suppressants have been developed, but many may compromise the performance of asphalt binder, which shortens the service life of asphalt pavement. This study aims to investigate the performance of a novel fume suppressant, namely oil-absorbing organogel polystyrene-stearyl methacrylate (P(S-SMA)), which can reduce the construction

fumes of asphalt binder while maintaining good rheological performance. The results of the Fourier Transform Infrared Spectroscopy (FT-IR), Fluorescence Microscopy (FM) and asphalt fume mass tests showed that adding P(S-SMA) can improve the aging resistance of asphalt binder and reduce the particles (⩾1 μm) and volatile organic compounds (VOCs) released up to 19.6 % and 30.4 % within 1 h, respectively. The rheological test results indicated that P(S-SMA) could effectively improve the viscoelastic properties, high-temperature performance and fatigue resistance of asphalt binder due to the combination of "supporting" and "hardening" effects after adding P(S-SMA). With 5% P(S-SMA) added, elastic and viscosity properties were increased by 90.6 % and 25.3 % and fatigue life was increased by 38.9 % and 26.4 % at the strain levels of 2.5% and 5%, respectively. This study proved the feasibility of using P(S-SMA) as a novel performance-enhancing fume suppressant of asphalt binder.

Keywords: Oil-absorbing organogel; Asphalt fumes; Modified asphalt binder; Microscopic analysis; Rheological properties

1. Introduction

Modified asphalt binders are widely used in pavement construction as a high-performance binder. The commonly used modifiers can be divided into various groups, such as polymer, biomass, fiber, etc. However, the production and construction processes of asphalt binder can generate a substantial amount of fumes (mainly composed of carbon oxides, sulfur oxides, nitrogen oxides[1], particles [2] and volatile organic compounds, VOCs)[3] because of the volatilisation and chemical reaction of asphalt components[4, 5] leading to air pollution[1, 6] and health risks to workers[7, 8]. Therefore, the addition of fume suppressants with physical suppression (obstruction, isolation, gap adsorption, etc.) or chemical suppression (chemical

blocking and carrier gas suppression) function[9, 10] is currently the primary solution, such as expanded graphite[11], active carbon[12], melamine[13], nano calcium carbonate[14], flame retardants[15], layered silicates[16, 17], etc. However, most of the suppressants may compromise the performance of the asphalt binder due to changes in the asphalt components or poor compatibility with the binder and initial modifiers[11-14]. In addition, compounding the conventional asphalt modifiers with suppressants to produce the modified asphalt binder would lead to a more complex production process and higher costs compared with using single modifier. Therefore, developing high-performance and multi-functional asphalt modifiers may lead to significant environmental, engineering and economic benefits.

As one kind of organogels, the oil-absorbing organogel has a three-dimensional network structure that allows it to absorb liquid organics, including esters, and expand its volume[18, 19]. Depending on the polarity of the constituent monomers, different oil-absorbing organogels can absorb the corresponding types of organic[19, 20]. Therefore, it has been applied to purify organic wastewater, crude oil spills, etc. In addition, the oil-absorbing organogel has a high chemical/thermal stability due to the high degree of cross-linking[19, 21], which are the desired characteristics of asphalt modifiers. However, the selection of monomers for the oil-absorbing organogel is critically important considering the complex chemical composition of asphalt[22].

In this study, to investigate the effect of oil-absorbing organogel as a fume suppressant on the asphalt binder performance, the polystyrene-stearyl methacrylate (P(S-SMA)) that can absorb asphalt components was synthesized. Then, it was used as a modifier to prepare the modified asphalt binder. Microscopic characterizations of P(S-SMA) were conducted by the Fourier Transform Infrared Spectroscopy (FT-IR), Thermogravimetric Analyzer (TGA) and swelling degree tests. Microscopic characteristics of P(S-SMA) modified asphalt binders were obtained

by the FT-IR, Fluorescence Microscopy (FM) and asphalt fume (fume particle and VOCs collection and Gas Chromatography-Mass Spectrometry, GC-MS) tests. The rheological performance of P(S-SMA) modified asphalt binders were determined by the dynamic shear rheological (DSR), performance grading (PG), multi-stress creep recovery (MSCR) and linear amplitude sweep (LAS) tests.

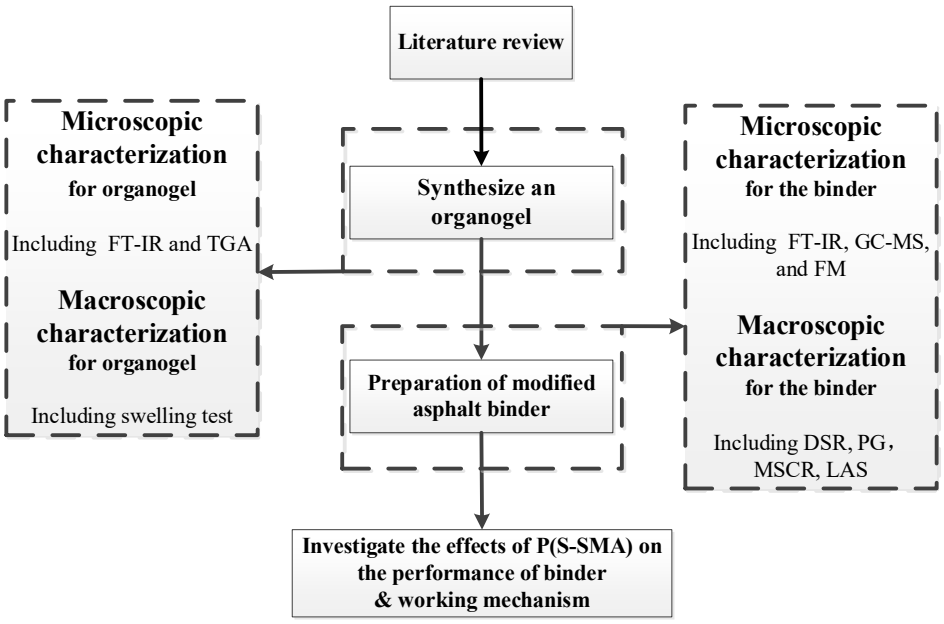

Fig. 1. Flowchart of research program

2. Materials and Methods

2.1 Testing materials

To prepare the P(S-SMA), Styrene (AR), Stearyl Methacrylate (SMA, AR) and Ethylene Glycol Dimethacrylate (EGDMA, AR) were used as the monomers and cross-linker, respectively. Boron Peroxide (BPO, AR) was used as the initiator. Benzene (AR) was used as the solvent which can supply the liquid environment for the reaction. To prepare the P(S-SMA) modified asphalt binders, the AH-90[#] with a penetration grade of 80/90 was used as the base asphalt binder. Dichloromethane (HPLC) was used as the solvent in the GC-MS test to absorb the organic fumes

released from the asphalt binder. The above materials can be used directly without special treatment.

2.2 Preparation of P(S-SMA)

SMA (2.36 g), styrene (3.64 g), EGDMA (0.102 g), BPO (0.092 g) and benzene (3 g) were added to a 50 mL beaker. After that, nitrogen (N_2) was introduced into the mixed solution for 10 min to remove the excess air. The beaker was then sealed and placed in a 75 °C oven for 6 h to obtain P(S-SMA). Finally, the P(S-SMA) was placed in a rotary evaporator and dried at 5 kPa and 75 °C to remove the contained benzene. The dried P(S-SMA) was crushed into powders (diameter mainly from 20-50 um) by the pulverizer, which can be used as the modifier.

During the reaction (Fig. 2), the monomers were dispersed in the benzene solvent. Styrene and SMA constituted the polymer molecular chains according to the addition reaction of carbon-carbon double bonds (C=C). At the same time, the EGDMA linked different chains by the same reaction, thus forming the three-dimensional spatial structure with many voids. At the same time, the retractive octadecyl groups of SMA were locked in the voids and could extend or contract with the changing amount of solvent (benzene).

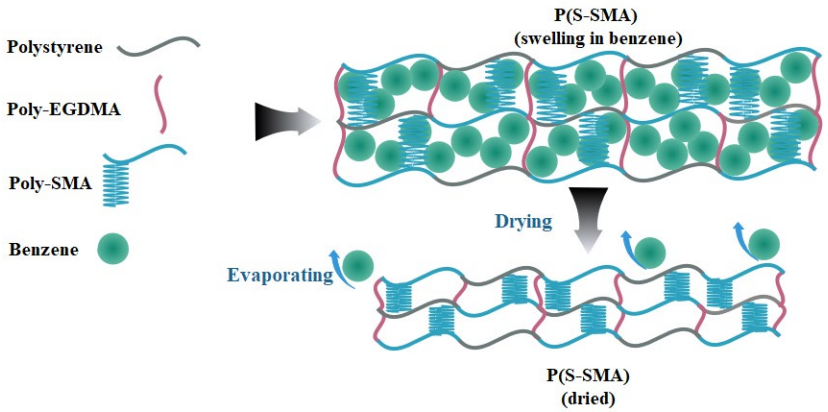

Fig. 2. Structural changes of P(S-SMA) before and after drying

2.3 Preparation of P(S-SMA) modified asphalt binder

The preparation process[23, 24] of P(S-SMA) modified asphalt binder is illustrated in Fig. 3. The base asphalt was heated in an oven at 130 °C for 2.5 h to remove the moisture. Afterwards, P(S-SMA) powder was added to the asphalt with different percentages and sheared by a high-speed shear emulsifier (5,000 rpm) at 140 °C for 40 min. Finally, the asphalt was cured in an oven at 135 °C for 1.5 h to obtain P(S-SMA) modified asphalt. To minimize the errors due to the preparation process, the control group (base asphalt binder) was also prepared in the same way except for adding P(S-SMA). The compositions and label names of the asphalts evaluated in this study are shown in Table 1. The lower temperature required for preparing P(S-SMA) modified asphalt than the traditional polymer modified asphalt (normally more than 160 °C)[23] also helps reduce the asphalt fumes and energy consumption during asphalt binder production. Considering the cost of P(S-SMA), the addition of it is up to the 5 % (less than 15% of the base binder cost).

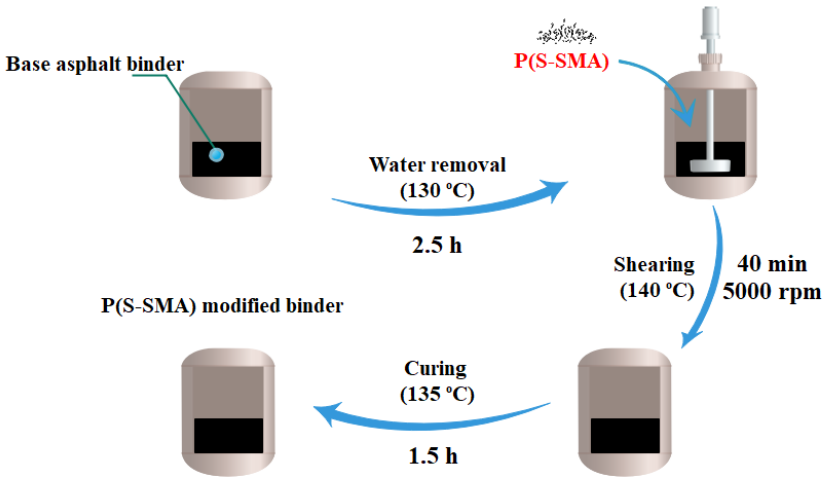

Fig. 3. Preparation process of P(S-SMA) modified asphalt binder

Table 1. Compositions of different types of asphalt binder

Number	P(S-SMA) content (wt %)	Type	Simplified name
1	0	Base asphalt binder	Base
2	1	1% P(S-SMA) modified binder	1% P(S-SMA)
3	3	3% P(S-SMA) modified binder	3% P(S-SMA)
4	5	5% P(S-SMA) modified binder	5% P(S-SMA)

2.4 Characterization and Performance analysis of P(S-SMA) and modified binders

2.4.1 Microscope characterizations of P(S-SMA)

Firstly, the FR-IR test (Perkin Elmer spectrum 100, PerkinElmer Co., Ltd.), which can analyze the chemical composition of materials, was used for both monomers and P(S-SMA) to verify the successful synthesis and analyze the chemical composition of P(S-SMA). After that, the TGA test (Mettler TGA/DSC3+, METTLER TOLEDO) that can evaluate the thermodynamic properties of materials was conducted on P(S-SMA) to analyze the thermal stability of it according to calculate the initial decomposition temperature of P(S-SMA). Moreover, the swelling test, which is a typical method to analyze the absorption ability of the absorptive material, was used to evaluate the properties of the P(S-SMA) according to the swelling degree Q (Eq. 1) [25]. Because of the complex chemical composition of asphalt binder, it can be typically divided into four fractions[26, 27], i.e. saturates (S), aromatics (A_r), resins (R) and asphaltene (A_s). In this study, a known mass of P(S-SMA) was added to each fraction and placed in an oven at 160 °C for 6 h. Afterwards, the P(S-SMA) was extracted, and its mass was measured after wiping off the asphalt component remaining on the surface.

$$Q = \frac{m_{wet} - m_{dry}}{m_{dry}} \quad (1)$$

where m_{wet} represents the mass of P(S-SMA) after immersion and m_{dry} represents the initial mass of P(S-SMA) before immersion.

2.4.2 Microscope characterizations of P(S-SMA) modified binders

Firstly, the FT-IR test (Perkin Elmer spectrum 100, PerkinElmer Co., Ltd.) was also conducted on the base and P(S-SMA) modified binders to analyze the chemical composition changes of modified binders before and after adding P(S-SMA) and in different ageing states. Moreover, the FT-IR test results were further used to evaluate the anti-aging properties of the modifed binder.

Previous studies indicated that in the infrared spectrum of asphalt binder, the band ranging from 600 to 1,300 cm^{-1}, also known as the fingerprint region, is more complex, as the position, shape, and intensity of the absorption peaks mainly depend on the components of binder[28]. In contrast, the 1,300 to 4,000 cm^{-1} band, known as the functional group region, is more straightforward and stable[29]. By comparing the infrared spectra of the positions and intensities of the absorption peaks of common functional groups before and after ageing, the changes in the components of asphalt binder under different ageing conditions can be obtained[30]. Previous studies[31, 32] have shown that the oxygen-containing functional groups of the asphalt binder increase significantly after ageing, mainly the characteristic carbonyl (C=O) peak at 1,670 cm^{-1}, generated by the reaction of C=C and oxygen with the temperature/light impact, and the characteristic sulfoxide (S=O) peak at 1,030 cm^{-1}, caused by the reaction of polar molecules of the binder with sulfurized organics. The carbonyl index (CI) and the sulfoxide index (SI) [30] usually represent the content of characteristic functional groups, and the changing rate of CI and SI (R_{CI} and R_{SI}) can be used to express the changes in content of characteristic functional groups before and after ageing. The corresponding equations are shown in Eq. (2-5).

$$CI = \frac{A_{C=O}}{A_{C-H}} \tag{2}$$

$$SI = \frac{A_{S=O}}{A_{C-H}} \tag{3}$$

$$R_{CI} = \frac{CI_{PAV} - CI_{Pre}}{CI_{Pre}} \times 100\% \tag{4}$$

$$R_{SI} = \frac{SI_{PAV} - SI_{Pre}}{SI_{Pre}} \times 100\% \tag{5}$$

where $A_{C=O}$ represents the C=O absorption peak area, $A_{S=O}$ represents the S=O absorption peak area, A_{C-H} represents the C-H absorption peak area, CI_{Pre} and CI_{PAV} represent the original and

long-term aged states of CI, respectively, and the SI_{Pre} and SI_{PAV} represent the original and long-term aged states of SI, respectively.

In addition, the FM test (IMAGER. Z2, Carl Zeiss AG) was used to observe the P(S-SMA) in asphalt binder at different ageing levels, which can analyze the Morphological changes of P(S-SMA) during the production and aging processes of the modified binder.

Finally, the asphalt fume test was used to analyze the fume-inhibiting effect of P(S-SMA) on particles and VOCs emission at a high temperature[33]. The binder (50 g, dried) was placed in a flask (100 ml) and then heated and stirred at 165 ºC for 1h. Through an air pump, dry air with the same flow rate (2.5 L/min) was blown into the flask. After that, the released fume was filtered by the glass fibre film (Whatman GF/B, aperture size: 1μm) and then absorbed by the organic solvent (DCM, for collecting the VOCs, 60 ml). By comparing the film mass changes of different binders, the particle mass changes can be measured. According to the GC-MS test (Agilent 7890B GC/5977A MSD), the concentration of VOCs of different binders can be analyzed. The splitless mode was used for the separation by an Agilent J&W Scientific HP-5ms column (30 m × 0.25 mm i.d.,0.25-μm film thickness, (5%-phenyl)-methylpolysiloxane coated), the purge to split vent times were 0.75 min with a flow of 20 ml/min, and SCAN mode was used for the acquisition (50 to 550 AMU). Fig. 4 shows the set-up program of the GC-MS test. The initial temperature was 40 ºC for 1 min, which was increased to 85 ºC at 15 ºC/min and held for 3 mins, and then to 110 ºC at 5 ºC/min and held for 2 mins, and to 200 ºC at 3 ºC/min and then to 300 ºC at 10 ºC/min and held for 8 mins. To improve the accuracy of GC-MS test results, the solvents were concentrated at 10 ml by nitrogen blowing and the injection volume was 1 μL.

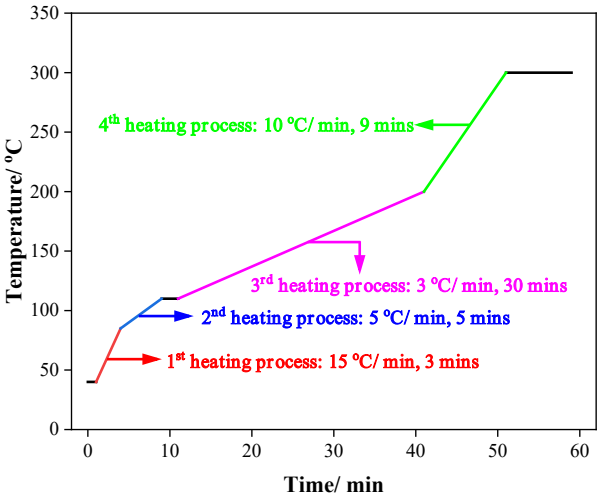

Fig. 4. Set-up program of the GC-MS test

2.4.3 Performance analysis of P(S-SMA) modified binders

Firstly, the DSR test (DHR-2, TA Instrument) was conducted to analyze the effect of the P(S-SMA) on the viscoelastic properties of the base asphalt binder. According to the American Association of State Highway and Transportation Officials (AASHTO) specification of DSR test (AASHTO T315)[34], various parameters related to asphalt rheological properties at different temperatures are obtained. The complex modulus (G^*), storage modulus (G'), loss modulus (G'') and phase angle (δ) represents the asphalt binder properties of resisting deformation, elastic, viscous and the ratio between the viscous and elastic properties, respectively. The relationships among G^*, G', G'' and δ are shown in Eq. 6 and 7[34]. The tests were conducted by frequency sweep using 25 mm standard plates (0.1-10 Hz) at different temperatures (46-76 °C) with a temperature-increasing interval of 6 °C.

$$G' = |G^*| \cos\delta \quad (6)$$

$$G'' = |G^*| \sin\delta \quad (7)$$

In addition, the PG test (DHR-2, TA Instrument) was conducted to analyze the effect of the P(S-SMA) on the high-temperature performance of the base asphalt binder. According to the

AASHTO specification of PG test (AASHTO M320)[35], all asphalt binders were graded by calculating the rutting factor (RF) at the original and short-term aged states as shown in Eq. 8, The G^* and δ represent the complex modulus and phase angle of binder at the same frequency (10 rad/s), respectively. The maximum temperature that corresponding RF of asphalt binder meets the demands (more than 1.0 kPa and 2.2 kPa at original and short-term aged states, respectively) is the performing grade of the binder.

$$RF = \frac{|G^*|}{\sin\delta} \quad (8)$$

After that, the MSCR test (DHR-2, TA Instrument) was conducted to analyze the effect of the P(S-SMA) on the rutting resistance of the base asphalt binder. Studies have proven that errors could occur when using RF to judge the rutting resistance of polymer-modified asphalt binder because the polymer modifiers (such as SBS, SBR, etc.) have good elastic properties[24]. Since P(S-SMA) is also a polymer material, the AASHTO specification of the MSCR test (AASHTO T350)[36] was chosen for a more accurate analysis of the rutting resistance of modified binders. The test temperature was 64 °C, and the stress were 0.1 kPa (20 loading cycles and the first 10 cycles are for conditioning the specimen) and 3.2 kPa (10 loading cycles) with 25mm standard plates used, respectively. Based on the peak strain (γ_p), the residual strain (γ_{nr}) and the loading stress (τ) in each cycle of the MSCR test results, the recovery rate (R), representing the elastic resilience of the asphalt binder, and the creep compliance (J_{nr}), representing the unrecoverable deformation of asphalt binder accumulated by the external forces, can be calculated using Eq. 9 and 10 [36], respectively.

$$R = \frac{\gamma_p - \gamma_{nr}}{\gamma_p - \gamma_0} \times 100\% \quad (9)$$

$$J_{nr} = \frac{\gamma_p - \gamma_{nr}}{\tau} \quad (10)$$

Finally, the LAS test (DHR-2, TA Instrument) was used to analyze the effect of the P(S-SMA) on the fatigue resistance of the base asphalt binder. The AASHTO specification of LAS test (AASHTO T391) was conducted on long-term aged asphalt binder specimens[37]. The test temperature was 25 ^{o}C, and 8 mm standard plates were used. The viscoelastic continuum damage (VECD) curves were calculated based on the test results, and the theoretical fatigue life of 2.5% ($N_{f2.5}$) and 5% (N_{f5}) strain were calculated.

3. Results and Discussion

3.1 Microscopic characterization of P(S-SMA)

3.1.1 FT-IR test

Fig. 5 shows the FT-IR spectra of P(S-SMA), SMA, EGDMA, and styrene. It can be found that the styrene spectrum has three peaks at 1,493.11 cm^{-1}, 1,601.10 cm^{-1} and 1,636.04 cm^{-1}, representing the absorption peaks of the benzene ring skeleton[38], while 1,636.04 cm^{-1} also corresponds to the C=C stretching vibration absorption peak[23, 39]. The SMA and EGDMA spectra have peaks at 1,721.69 cm^{-1} and 1,164.32 cm^{-1}, which are due to the C=O and C-O stretching vibrational absorptions[40, 41], respectively, and both have the C=C stretching vibrational absorption peak at 1,636.04 cm^{-1}. Comparing the spectra of the P(S-SMA), SMA, EGDMA and styrene, it can be found that the disappearance of the C=C stretching vibration absorption peak at 1,636.04 cm^{-1} disappeared in the spectrum of P(S-SMA), which indicates that P(S-SMA) was synthesized due to the addition reaction between the C=C groups of SMA, EGDMA and styrene. The disappeared C=C absorption peak also proves a high degree of reaction, which ensures the high chemical stability of P(S-SMA).

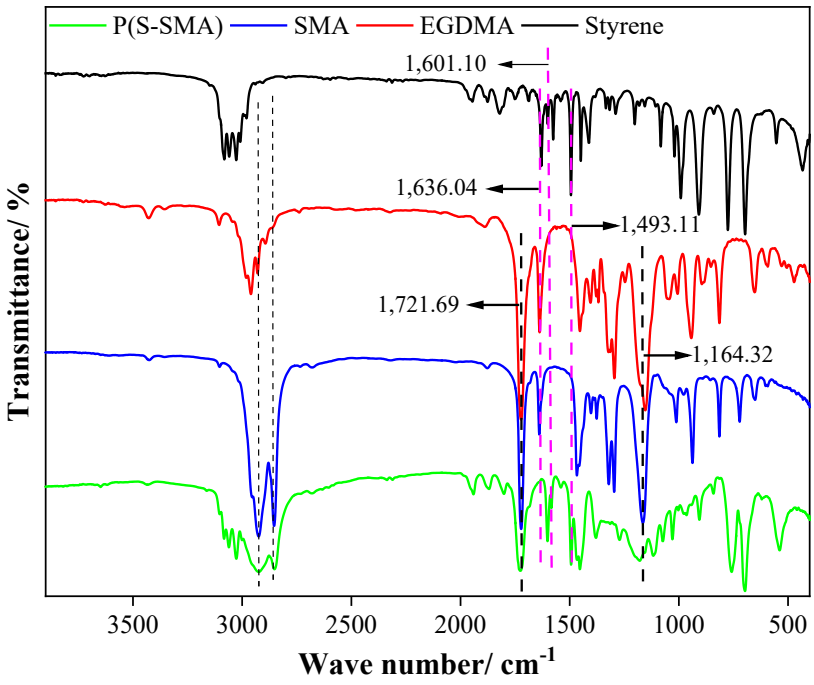

Fig. 5. FT-IR spectra of P(S-SMA) and related monomers

3.1.2 TGA test

According to the standard specification of asphalt pavement construction[42], the temperature range of preparation and construction processes of the modified asphalt binder is typically 160 °C - 190 °C. The asphalt modifier with a lower decomposition temperature than the requirement can cause the decomposition of itself during the application. Fig. 6 shows the TGA curve of P(S-SMA). It can be seen that the characteristic decomposition temperature of P(S-SMA) was 363.09 °C, which indicates that P(S-SMA) has suitable thermal stability and can meet the requirements of modifiers in the production and construction processes of modified asphalt materials.

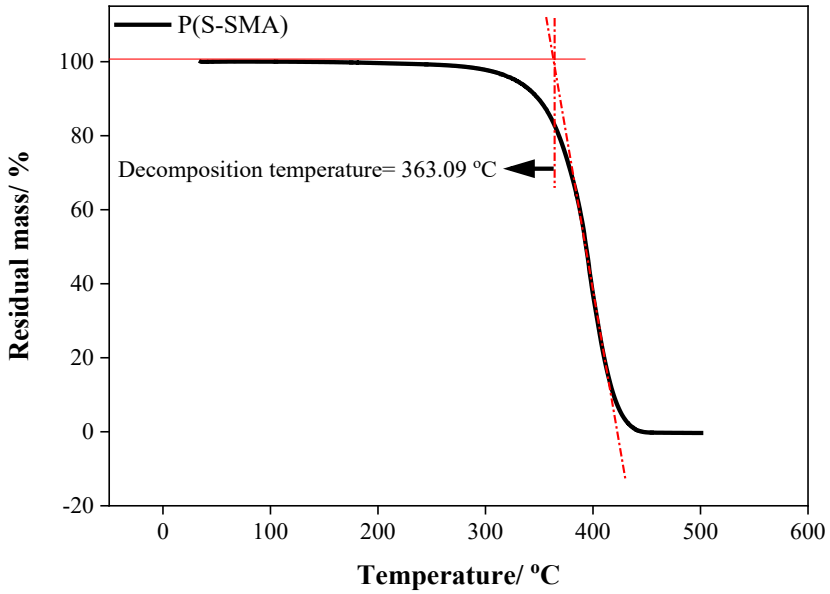

Fig. 6. TGA test result of P(S-SMA)

3.1.3 Swelling degree test

Fig. 7 and Table 2 show the swelling test results of P(S-SMA) in different asphalt fractions. It can be found that P(S-SMA) had different mass and volume changes after absorbing saturates, aromatics, resins, and asphaltene with swelling degrees of 0.345, 0.344, 0.712 and 0.026, respectively. P(S-SMA) had the highest absorption ability of resins, similar absorption abilities of saturates and aromatics, and a very low absorption ability of asphaltene.

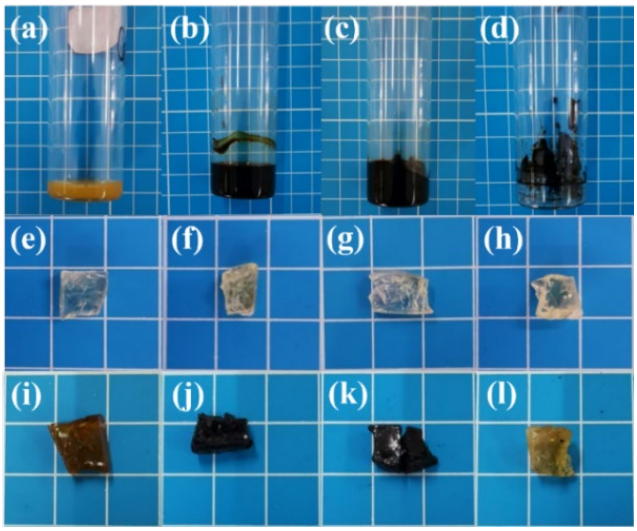

Fig. 7. Volume changes of P(S-SMA) before and after immersion: (a) saturates; (b) aromatics; (c) resins; (d) asphaltene; (e-h) P(S-SMA) before immersion and (i-l) after immersion

Table 2. Q of P(S-SMA) in different asphalt fractions

Type	m_{dry}/ g	m_{wet}/ g	Q
S	0.2039	0.2742	0.345
A_r	0.1691	0.2273	0.344
R	0.1558	0.2666	0.712
A_s	0.2056	0.2109	0.026

When added in asphalt binder, a certain amount of binder factions could be stored in the voids of P(S-SMA). At the same time, the contracted octadecyl groups of SMA in the voids are infiltrated and gradually expanded in the absorbed factions, thus causing the swell of the voids volume, as Fig. 8 illustrates. This change also leads to a gradual decrease in the P(S-SMA) network density, so that its mechanical strength gradually decreases and is prone to deform. However, because of the 3D structure and the filling of the absorbing materials, the swelled P(S-SMA) can occur elastic deformation (within the damage limits)[43].

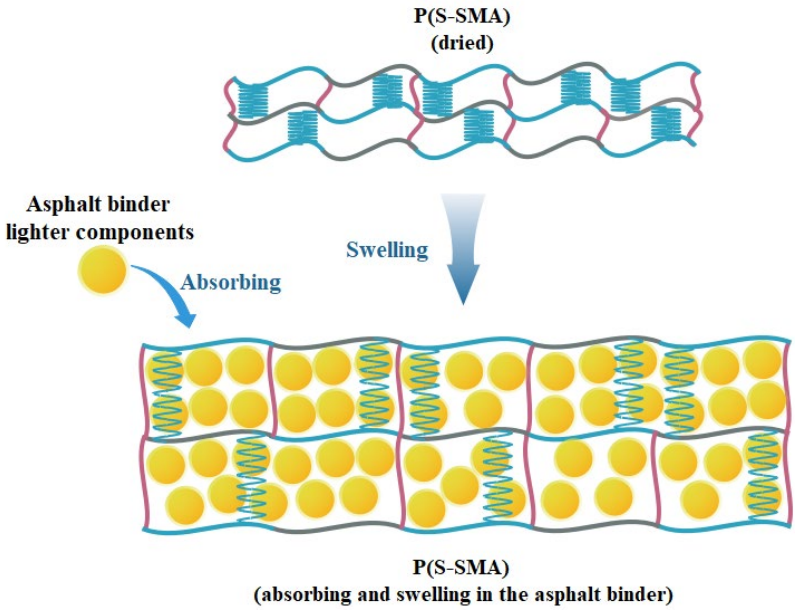

Fig. 8. Structural changes of P(S-SMA) before and after swelling in lighter components of asphalt binder

3.2 Microscopic characterization of P(S-SMA) modified asphalt binder

3.2.1 FT-IR test

Fig. 9 shows the FT-IR spectra of different asphalt binders before and after aging. It can be found that the FT-IR spectra of 5% P(S-SMA) modified asphalt binder did not show any new absorption peaks compared with the base asphalt binder, indicating that no new chemical reaction had occurred after the addition of P(S-SMA), i.e., the modification of P(S-SMA) to asphalt binder should be physical. It can also be noticed that no new absorption peaks appeared, except for changes in the area of some of the absorption peaks, after aging for both binders, indicating that P(S-SMA) does not react with the components of the binder after ageing. These FT-IR test results suggest that P(S-SMA) has good chemical stability, which is consistent with the findings of the FT-IR tests of P(S-SMA).

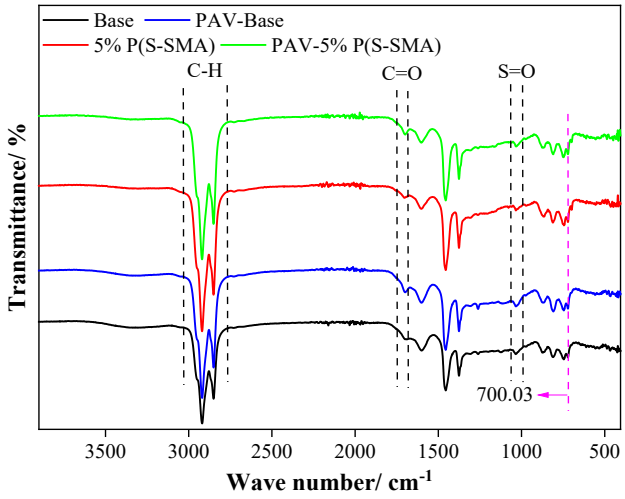

Fig. 9. FT-IR spectra of different asphalt binders in original and long-ageing states

Based on the test results in Fig. 9, the CI and SI were calculated for the two asphalt binder samples in their original and long-term aged state. The calculations are shown in Table 3, which can be found that CI and SI of both asphalt binders increased after ageing. Base asphalt binder has more increase in CI and SI, with R_{CI} and R_{SI} reaching 148.7 % and 67.2 %, respectively, while the R_{CI} and R_{SI} of 5% P(S-SMA) modified asphalt binder were 71.9 % and 46.0 %, respectively, which were 51.6 % and 31.6 % less than those of base asphalt binder, respectively. Meanwhile, the values of CI and SI for the 5% P(S-SMA) modified asphalt binder were smaller than the base asphalt binder in both the original and long-term aged states. These test results indicated that the addition of P(S-SMA) could reduce the content of C=O and S=O, i.e., slow down the oxidation reaction rate between O_2 and C=C and S, thus improving the aging resistance (thermal and oxygen) of the asphalt binder. In addition, the effect of P(S-SMA) on C=C is more pronounced, since P(S-SMA) absorbs more components of asphalt that are susceptible to oxidation (especially those containing C=C), thus inhibiting the oxidation of these components during the ageing process.

Table 3. CI and SI of different asphalt binders

Type	A_{C-H}	$A_{C=O}$	$A_{S=O}$	CI	R_{CI}/ %	SI	R_{SI}/ %
Base	3525.311	41.835	49.096	0.01187	148.7	0.01393	67.2
PAV-base	2685.431	79.263	62.537	0.02952		0.02329	
5% P(S-SMA)	4151.237	43.854	40.643	0.01056	71.9	0.00979	46.0
PAV-5% P(S-SMA)	4073.522	73.991	58.221	0.01816		0.01429	

3.2.2 FM test

Fig. 10 shows the FM images of different asphalt binders in the original states with X100 and X400 magnifications. As can be found in Fig. 10(a), the surface of the base asphalt binder was smooth, and no material with fluorescent phenomena appeared. After adding P(S-SMA), shown in Fig. 10(b-d), some powder with green fluorescence was evenly dispersed and continued to increase in the asphalt binder.

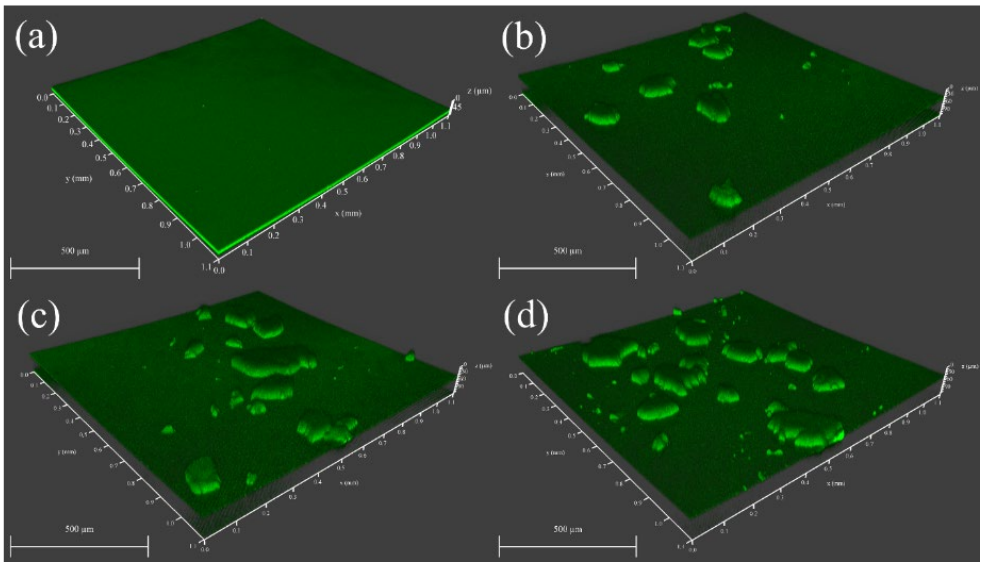

Fig. 10. FM test results for different original asphalt binders with various addition of P(S-SMA): (a) base, (b) 1% P(S-SMA), (c) 3% P(S-SMA) and (d) 5% P(S-SMA)

Fig. 11 shows the FM images of the modified asphalt binders in the original and long-term aged states. From Fig. 11(a and b), it can be found that the P(S-SMA) continued to be present in the modified asphalt binder after ageing treatments. At the same time, there is no significant change

316 in the distribution density of P(S-SMA) between the pristine and long-term aged states. In
317 addition, the volume of P(S-SMA) in the long-term aged state modified asphalt binder increased
318 compared with the original state. The same phenomenon can also be observed in the images of
319 the 3% and 5% P(S-SMA) modified binders (Fig. 11(c-f)), which are consistent with the findings
320 of the swelling degree tests. These test results indicate that P(S-SMA) cannot decompose in the
321 binder during the preparation and ageing process, which means that the material has sufficient
322 thermal stability in asphalt materials during practical applications. In addition, the swelling of
323 P(S-SMA) could be attributed to the absorption of light components of binder during the
324 preparation and ageing process.

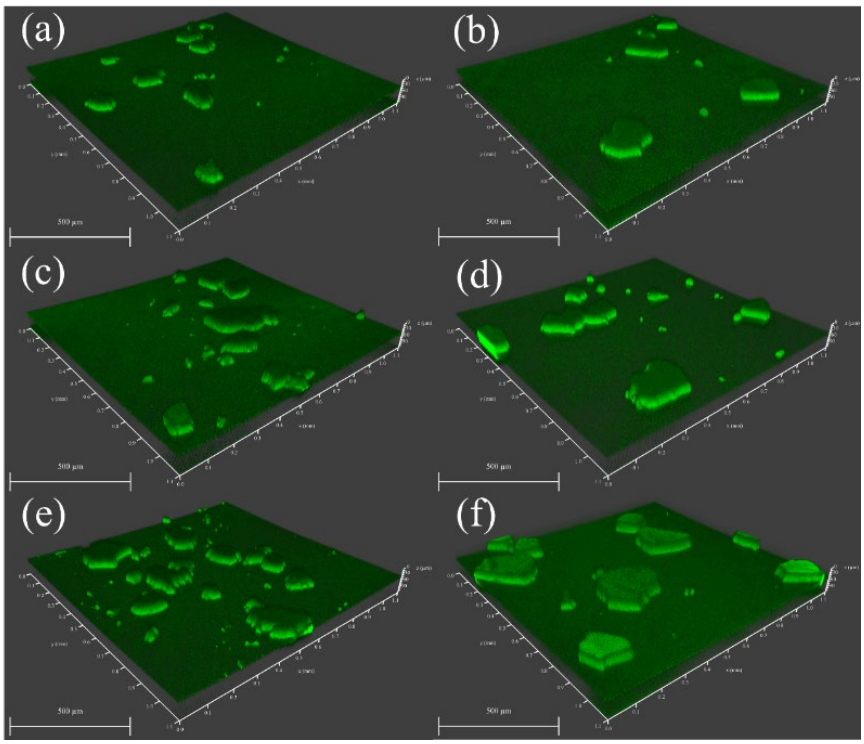

325

326 **Fig. 11.** FM test results for different asphalt binders in different states: (a) 1% P(S-SMA), (c) 3%
327 P(S-SMA) and (e) 5% P(S-SMA) were at the original state and (b) 1% P(S-SMA), (d) 3% P(S-
328 SMA) and (f) 5% P(S-SMA) were at the long-term aged state

329 **3.2.3 Asphalt fume test**

Table 4 shows the particle mass of different binders during the testing process. It can be found that the base binder has the largest particle mass, indicating the largest particle released during the heating process. Compared to the base binder, the particle mass of P(S-SMA) modified binder continued to decrease with the increasing amount of P(S-SMA), which reached 19.6 % decrease with 5% P(S-SMA) added. These results indicate that the P(S-SMA) can reduce particle release of asphalt binder.

Table 4. Particle mass of different binders

Binder type	Particle mass/ g	Changing rate/ %
Base	0.0542	--
1% P(S-SMA)	0.0517	4.6
3% P(S-SMA)	0.0483	10.9
5% P(S-SMA)	0.0436	19.6

Fig. 12, Table 5 and Table S1 (appendix) show the VOCs concentration of different binders, which can be dividied into chain hydrocarbons (Alkane, alkene, cycloalkanes, etc.), hydrocarbon derivatives (naphthene, aldehyde, etc.) and aromatic compounds (benzene, phenol, naphthalene, Indan, etc.). The chemicals represented by each peak were identified by MS library[44] (NIST14, match degree $\geqslant$70). The concentration of each chemical was represented by the corresponding peak abundance. It can be found in Fig. 12 and Table S1 and Table 5 that the base binder (Fig. 12(a)) has the highest peak abundance, which means the highest VOCs concentration. After adding the P(S-SMA), the peak abundance decreased, indicating a lower VOCs concentration. Among them, the 5% P(S-SMA) binder got the lowest total peak abundance by 30.4 % decrease. These results indicate the P(S-SMA) can reduce the VOCs released from asphalt binder. Moreover, the peak abundances of chain hydrocarbons and aromatic compounds have the biggest changes, indicating that the P(S-SMA) has the highest absorbing ability for them.

In summary, the reduced particle and VOCs mass indicate that P(S-SMA) can effectively reduce air pollution caused by the fume from heating asphalt materials. This effect can be enhanced by increasing the amount of P(S-SMA) added.

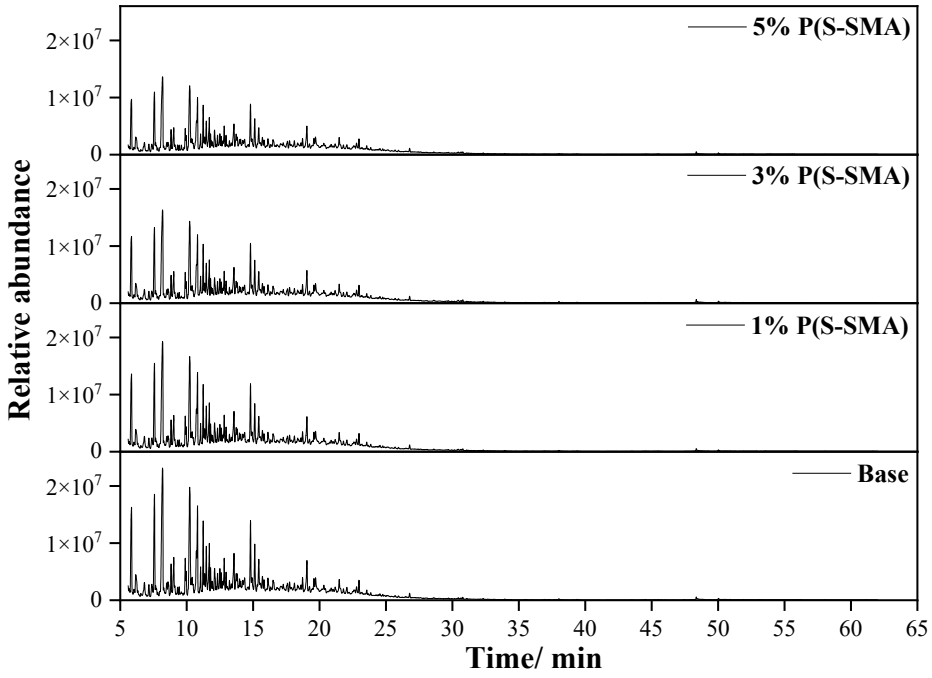

Fig. 12. GC-MS test results of different binders

Table 5. VOCs concentration of four asphalt binders

Chemical type	Base	1% P(S-SMA)		3% P(S-SMA)		5% P(S-SMA)	
	Relative abundance/ 10^5	Relative abundance/ 10^5	Changing rate/ %	Relative abundance/ 10^5	Changing rate/ %	Relative abundance/ 10^5	Changing rate/ %
Chain hydrocarbons	1448.2	1305.58	-9.85	1202.58	-16.96	1095.88	-24.33
Hydrocarbon derivatives	99.56	93.7	-5.89	87.78	-11.83	85.1	-14.52
Aromatic compounds	5574.26	4846.62	-13.05	4399.82	-21.07	3776.56	-32.25
Total	7122.03	6245.90	-12.3	5690.18	-20.1	4957.54	-30.4

3.3 Rheological performance tests of P(S-SMA) modified asphalt binder

3.3.1 DSR test

Fig. 13 shows the effect of the P(S-SMA) and the various amounts added on the G' of the base asphalt binder. A larger value of G' means a higher elastic property of asphalt binder. From Fig. 13(a), it can be found that G' of all four asphalt binders were increased with increasing loading frequency at the same temperature (46 °C). Among them, the G' of the base asphalt binder was the smallest. When the P(S-SMA) was added, the G' of the asphalt binder was increased and achieved the maximum with 90.6 % improvement when 5% P(S-SMA) was added. From Fig. 13(b), it can be found that at the same frequency (10 Hz), G' of all four asphalts were decreased with increasing temperature. Among them, the G' of the base asphalt was also the smallest, and it kept increasing with the increasing percentage of P(S-SMA). These results indicated that the addition of P(S-SMA) can effectively improve the elastic properties of asphalt binder.

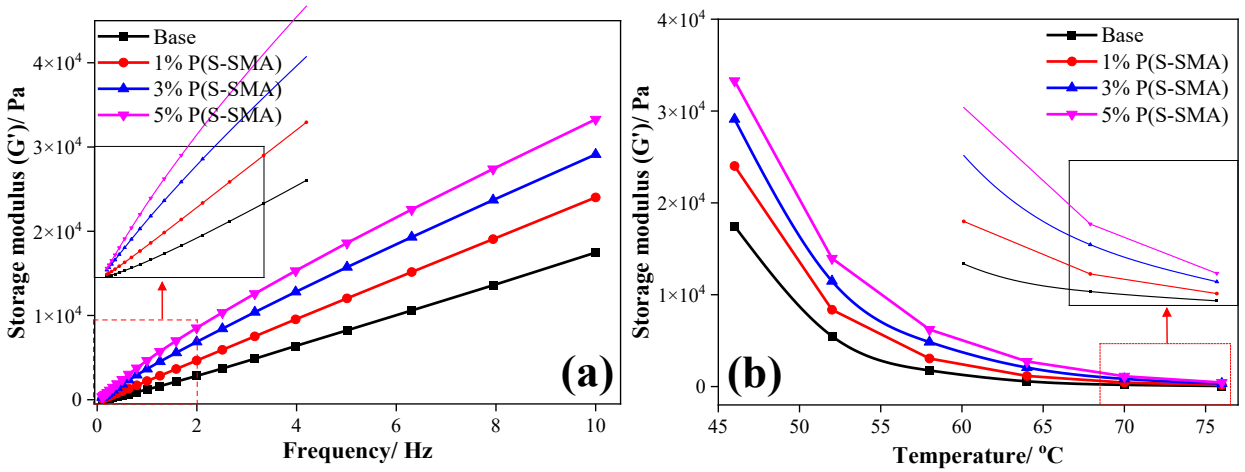

Fig. 13. Effect of the P(S-SMA) and the various amounts added on the G' of asphalt binders: (a) different test frequencies (0.1-10 Hz) at a constant temperature (46 °C) and (b) different test temperatures (46-76 °C) at a constant frequency (10 Hz)

Fig. 14 shows the effect of the P(S-SMA) and the various amounts added on the G" of base asphalt binder, similar to the relationship of G' between different asphalt binders. A larger value of G" indicates higher viscous properties of asphalt binder. From Fig. 14(a), it can be found that

G" of all asphalt binders also increased with the increasing loading frequency at the same test temperature (46 °C). The G" of base asphalt binder was again the smallest in the full range and improved when P(S-SMA) was added. The maximum increase of 25.3 % was achieved at 10 Hz when 5% P(S-SMA) was added. From Fig. 14(b), it can be found that at the same test frequency (10 Hz), G" of all asphalt binders decreased with the increasing temperature. The G" of base asphalt binder was also the smallest and improved when P(S-SMA) was added. These results indicate that the viscous properties of asphalt binder can be enhanced with the addition of P(S-SMA)

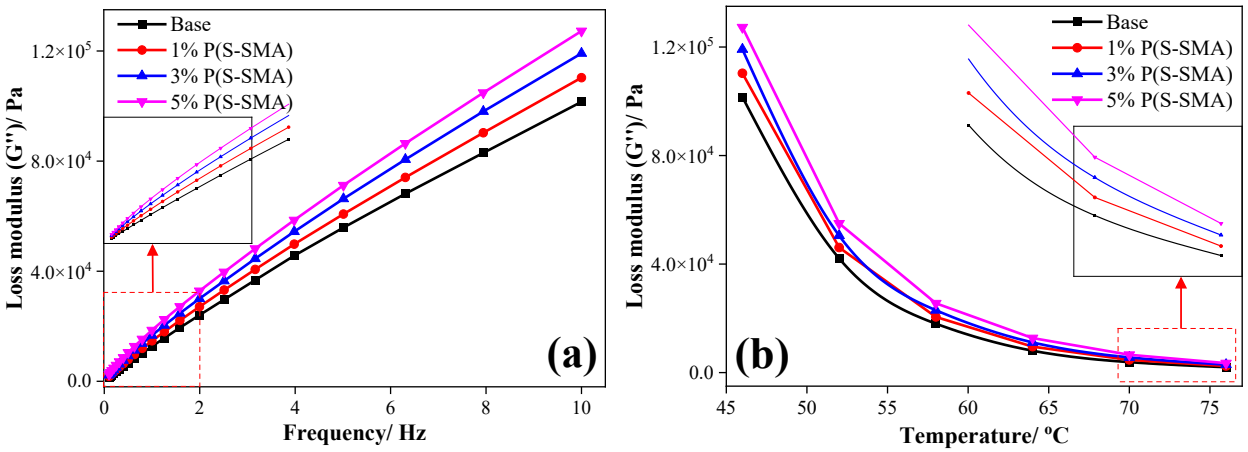

Fig. 14. Effect of the P(S-SMA) and the various amounts added on the G" of asphalt binders: (a) different test frequencies (0.1-10Hz) at constant temperature (46 °C) and (b) different test temperatures (46-76 °C) at a constant frequency (10 Hz)

Fig. 15 shows the effect of the P(S-SMA) on the δ of base asphalt binder. A larger value of δ represents a smaller proportion of elasticity in the asphalt binder compared to the viscosity. From Fig. 15(a), it can be found that at the same test temperature (46 °C), the δ of all asphalt binders decreased with the increasing loading frequency and the base asphalt binder had the largest δ. After P(S-SMA) added, the δ reduced and got the minimum value with 5% P(S-SMA) added.

From Fig. 15(b), it can be found that at the same test frequency (10 Hz), the δ of all four asphalt binders increased with the increasing temperature. Among different binders, the larger percentage of P(S-SMA), the smaller δ, indicating that P(S-SMA) can increase the proportion of elasticity of asphalt binder.

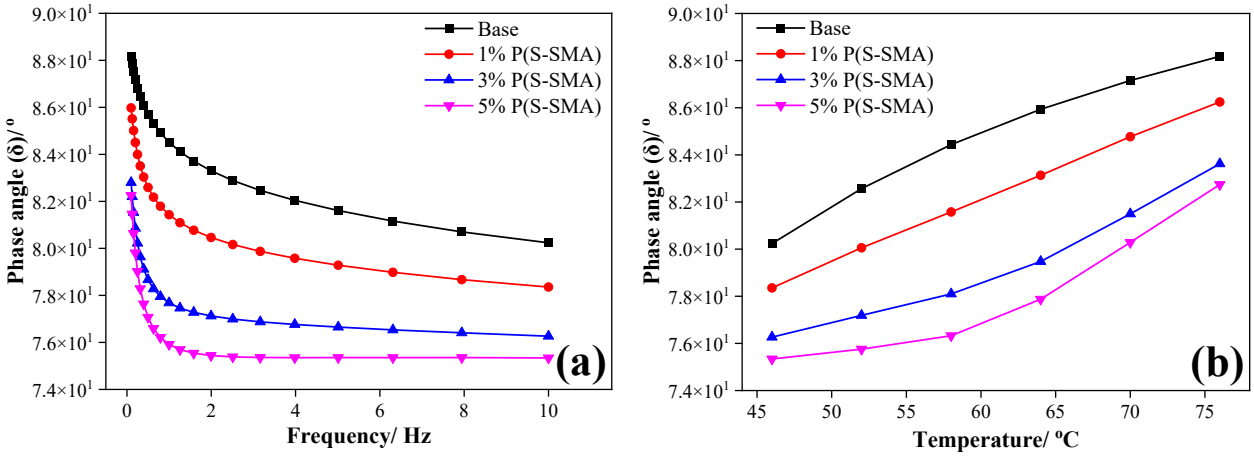

Fig. 15. Effect of the P(S-SMA) and the various amounts added on the tanδ of asphalt binders: (a) different test frequencies (0.1-10 Hz) at a constant temperature (46 °C) and (b) different test temperatures (46-76 °C) at a constant frequency (10 Hz)

In summary, P(S-SMA) has a significant effect on the viscoelastic properties of asphalt binder and a more significant effect on the elastic properties than the viscous properties. In addition, this effect could be enhanced by increasing the addition of P(S-SMA) (within the experimental range). This phenomenon would be caused by the interaction between the P(S-SMA) and asphalt components. Fig. 16 illustrates the relationship between the working mechanism of P(S-SMA) in asphalt binder. During the preparation process of modified asphalt binder, the P(S-SMA) can absorb the lighter components (saturates, aromatics and resins) of asphalt binder and swell. Meanwhile, the absorbed light components lead to an increased percentage of the heavy components in the asphalt binder. As a result, the flowability of the binder is reduced, which

could be reflected in the rheological tests as an increase in viscous properties. Thus, the combined "supporting" effect of the P(S-SMA) due to the filling in binder and "hardening" effect of the binder due to the change in composition contribute to the improved viscoelastic properties of the asphalt binder. In addition, the increase in the proportion of elastic properties of P(S-SMA) modified asphalt binder indicates that the "supporting" effect of P(S-SMA) is more pronounced. As a result of these changes, the P(S-SMA) modified asphalt realizes the process of "strengthening elasticity" and "strengthening viscosity", which leads to the effective improvement of asphalt performance.

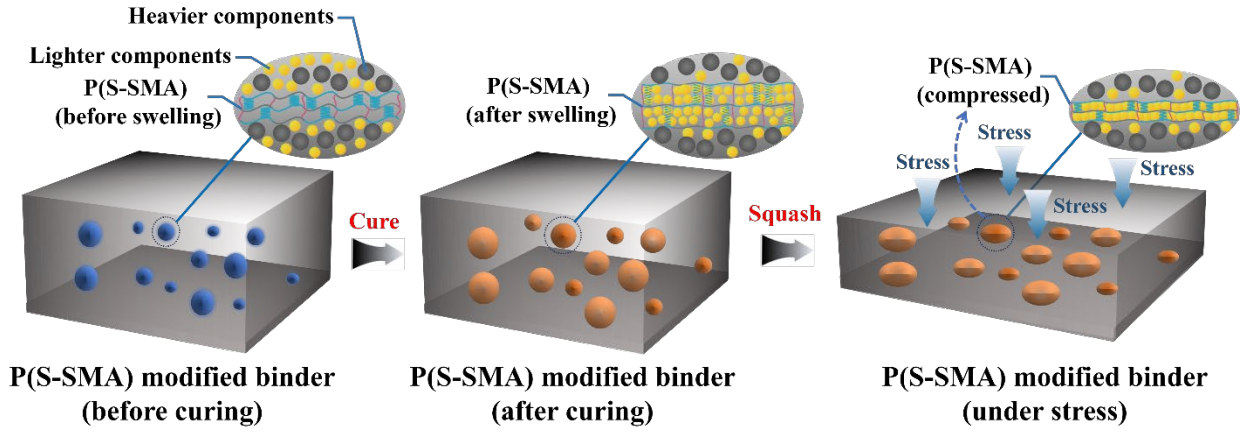

Fig. 16. Modification mechanism of P(S-SMA) in base asphalt binder

3.3.2 High-temperature PG test

Table 6 shows the RF of various asphalt binders in different ageing states. It can be found that the RF of the base asphalt binder gradually decreased as the temperature increased. In addition, the RF of the short-term aged sample was significantly greater than that of the original specimen at the same temperature, and the base asphalt binder met the requirements of PG 64. With the addition of P(S-SMA), the RF of the modified asphalt binder in both ageing states increased significantly. Also, with the amount of P(S-SMA) added increased, RF was increased and achieved the maximum with 5% P(S-SMA) added, which met the requirements of PG 70. These

test results indicate that the addition of P(S-SMA) can improve the high-temperature performance of the asphalt binder, and this effect can be enhanced with increasing amounts of P(S-SMA). These phenomena are also due to the combined "supporting" and "hardening" effects of P(S-SMA).

Table 6. RF of various asphalt binders in different ageing states

Temperature/ °C	Base	1% P(S-SMA)	3% P(S-SMA)	5% P(S-SMA)
	RF/ kPa	RF/ kPa	RF/ kPa	RF/ kPa
58	3.125	3.863	4.729	5.517
64	1.356	1.714	2.150	2.534
70	0.629	0.802	1.014	1.207
76	0.317	0.399	0.629	0.599
		RTFOT		
58	7.144	8.279	9.450	10.931
64	3.052	3.646	4.226	4.998
70	1.377	1.676	1.960	2.327
76	0.652	0.808	0.959	1.134
PG	64	64	64	70

3.3.3 MSCR test

Fig. 17 shows the MSCR test results of various binders at different stresses. It can be observed from Fig. 17(a) that the four asphalt binders showed a stepwise increase in strain with increasing loading cycles at the loading stress of 0.1 kPa, which is similar to the vehicle travel condition (intermittent loading) of the actual pavement. Among them, the total strain of the base asphalt binder was the largest. With the addition of P(S-SMA), the total strain was decreased, caused by the reduction in the residual strain at each testing cycle. As the amount of P(S-SMA) added increased, the residual and total strain continued to decrease at each loading step. Compared with the base asphalt binder, the total strain decreased 52.0 % when 5% P(S-SMA) was added. When the stress increased to 3.2 kPa, as shown in Fig. 17(b), the total strain for all four asphalt binders increased, caused by the increase in residual strain per cycle due to the loading stress increasing. Among them, similar to Fig. 17(a), the total strain of the base asphalt binder remained the largest

and decreased with P(S-SMA) added, which achieved the minimum with 45.7 % reduced after adding 5% P(S-SMA). These results indicate that the addition of P(S-SMA) can improve the resistance of the asphalt binder to deformation, and this effect can be enhanced with the increasing P(S-SMA) content.

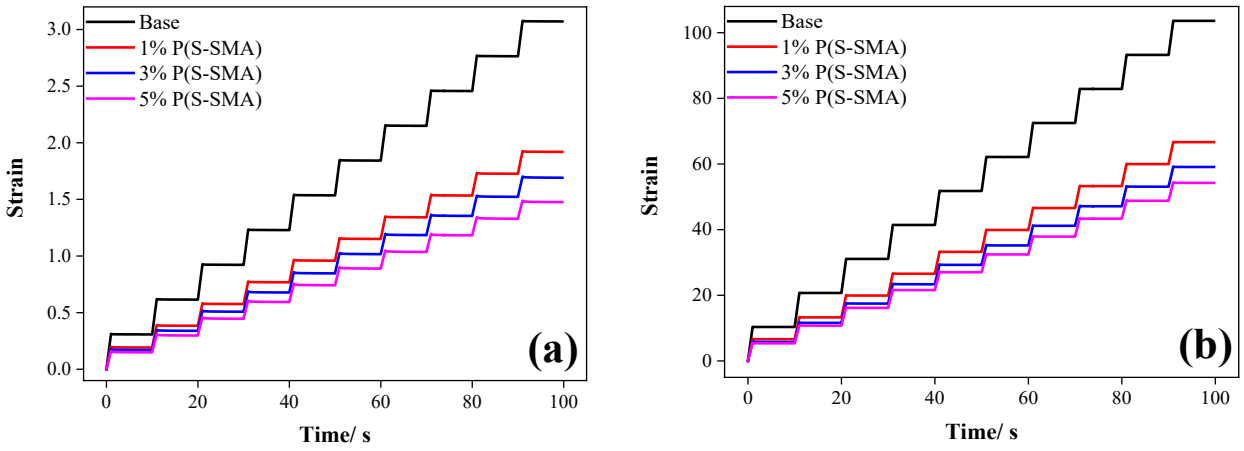

Fig. 17. Effect of the P(S-SMA) and various amounts added on the strain-time relations of different asphalt binders (64 °C): (a) 0.1 kPa and (b) 3.2 kPa

According to the test results in Fig. 17, the R and J_{nr} of various binders were calculated, as shown in Table 7. As can be found from Table 7, the $R_{0.1}$ of the base asphalt binder was the smallest at the test stress of 0.1 kPa. With the addition of P(S-SMA), the $R_{0.1}$ of asphalt binder was increased and continued increasing as more P(S-SMA) was added. The $R_{0.1}$ of the asphalt binder reached the maximum when 5% P(S-SMA) was added, which is a rise of 427.5 % compared to the base asphalt binder. After raising the stress to 3.2 kPa, the R of all four asphalt binders decreased, and alsothe base asphalt binder got the smallest value. When P(S-SMA) was added, the $R_{3.2}$ of asphalt binder was increased, which achieved the maximum with 785.0 % increase as 5% P(S-SMA) was added. These results indicate that adding P(S-SMA) can enhance

the elastic recovery properties (delayed elastic recovery) of the base asphalt binder. Furthermore, this effect can be improved by increasing the amount of P(S-SMA) added.

The J_{nr} of the base asphalt binder was the largest among the four binders at both stress levels, and adding P(S-SMA) reduced J_{nr}. These results indicated that P(S-SMA) can enhance the resistance to permanent deformation of the base asphalt binder, and this effect can be enhanced by increasing the P(S-SMA) content.

Table 7. R and J_{nr} of different asphalts at 0.1 kPa and 3.2 kPa (64°C)

Type/ Unit	Base	1% P(S-SMA)	3% P(S-SMA)	5% P(S-SMA)
$R_{0.1}$/ %	1.657	3.805	5.651	8.741
$R_{3.2}$/ %	0.366	1.485	2.259	3.239
$J_{nr0.1}$/ kPa^{-1}	3.072	1.920	1.707	1.444
$J_{nr3.2}$/ kPa^{-1}	3.238	2.083	1.892	1.681

In summary, the addition of P(S-SMA) can effectively improve the rutting resistance of the base asphalt binder, and this effect could continue to be increased as the amount of P(S-SMA) added increases. asphalt binder. The "hardening" effect of P(S-SMA) could help prevent asphalt binder from deforming when subjected to external forces, and the "supporting" effect could help the binder quickly recover from the deformation.

3.3.4 LAS test

Fig. 18 and Table 8 show the LAS test and corresponding VECD results of various asphalt binders, respectively. As can be seen from Table 8, adding P(S-SMA) could increase the fatigue lives of the base asphalt binder at both strain levels. When 5% P(S-SMA) was added, $N_{f2.5}$ and N_{f5} were increased by 38.9 % and 26.4 %, respectively. These test results indicated that adding P(S-SMA) can improve the fatigue resistance of asphalt binder, and this effect can be enhanced with the amount of P(S-SMA) added increases, which was also due to the combined "hardening" and "supporting" effects of P(S-SMA).

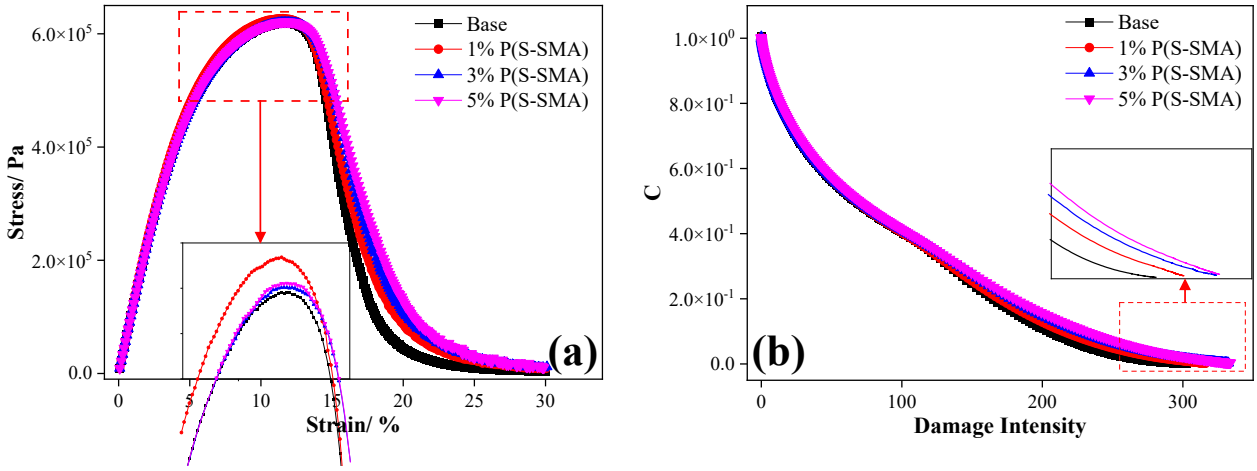

Fig. 16. Results of (a) LAS tests and corresponding (b) VECD curves for different asphalt binders

Table 8. Theoretical fatigue life (N_f) of four asphalt binders under different strains

Strain/ %	Base	1% P(S-SMA)	3% P(S-SMA)	5% P(S-SMA)
2.5	25180	28443	31993	34969
5	3540	3966	4289	4474

4. Conclusions

This study investigated the effect of a novel fume suppressant, the oil-absorbing gel P(S-SMA), on the rheological properties and fume release of asphalt binder. The following findings can be obtained based on the outcome of this study:

1. Micro- and macro-characterization analyses of P(S-SMA) proved that P(S-SMA) with better chemical and thermal stabilities can absorb the asphalt light components (saturates, aromatics and resins).

2. Micro-characterization analyses of modified asphalt binder proved that using P(S-SMA) as a modifier can enhance the aging resistance of asphalt binder and reduce particle mass and

VOCs emission of asphalt fume by 19.6 % and 30.4 %, respectively, at high temperatures with 5% addition.

3. The rheological test results showed that adding P(S-SMA) can improve the elastic and viscosity properties up to 90.6 % and 25.3 %, respectively, extend the fatigue life up to 38.9 % (2.5% strain) and 26.4 % (5% strain) and enhance the rutting resistance of asphalt binder, which are advantages compared to other fume suppressants. In addition, these effects can be strengthened with the increasing amount of P(S-SMA).

P(S-SMA) showed the above positive effects, because it can absorb the lighter components of asphalt, thus swelling and acting as a "supporting" effect in the asphalt. In addition, the reduction of the lighter components of the asphalt leads to an increase in the percentage of the heavier components and causes the "hardening" effect of asphalt. As a result of these changes, the P(S-SMA) modified asphalt has "strengthened elasticity" and "strengthened viscosity", leading to improved performance.

In summary, as a novel asphalt fume suppressant, P(S-SMA) showed positive modification effects on asphalt binder, providing advantages in environmental protection and pavement durability. However, the relationship between the oil-absorbing organogel properties and the asphalt binder performance needs more systematic research. In addition, the optimum P(S-SMA) content in asphalt mixture should be determined based on the trade-off of the production cost and performance of the modified asphalt binder.

Acknowledgements

This work was supported by the National Natural Science Foundation of China Joint Fund for Regional Innovation and Development [Grant No. U20A20315] and the Open Research Fund Program of Guangdong Key Laboratory of Urban Informatics [Grant No. SZU510292020050].

References

[1] C.A. Schreiner, Review of mechanistic studies relevant to the potential carcinogenicity of asphalts, Regulatory toxicology and pharmacology : RTP 59(2) (2011) 270-84.
[2] Y.J. Boom, M. Enfrin, S. Grist, F. Giustozzi, Recycled plastic modified bitumen: Evaluation of VOCs and PAHs from laboratory generated fumes, Science of The Total Environment 832 (2022) 155037.
[3] A. Fathollahi, C. Makoundou, S.J. Coupe, C. Sangiorgi, Leaching of PAHs from rubber modified asphalt pavements, Science of The Total Environment 826 (2022) 153983.
[4] X. Qin, S. Zhu, S. Chen, K. Deng, The mechanism of flame and smoke retardancy of asphalt mortar containing composite flame retardant material, Construction and Building Materials 41 (2013) 852-856.
[5] H. Rajabi, M. Hadi Mosleh, P. Mandal, A. Lea-Langton, M. Sedighi, Emissions of volatile organic compounds from crude oil processing - Global emission inventory and environmental release, The Science of the total environment 727 (2020) 138654.
[6] M.D. McClean, R.D. Rinehart, L. Ngo, E.A. Eisen, K.T. Kelsey, R.F. Herrick, Inhalation and Dermal Exposure among Asphalt Paving Workers, The Annals of Occupational Hygiene 48(8) (2004) 663-671.
[7] N. IARC Working Group on the Evaluation of Carcinogenic Risks to Humans, Some Industrial Chemicals, 2018.
[8] J. Fostinelli, E. Madeo, E. Toraldo, M. Sarnico, G. Luzzana, C. Tomasi, G. De Palma, Environmental and biological monitoring of occupational exposure to polynuclear aromatic hydrocarbons during highway pavement construction in Italy, Toxicology Letters 298 (2018) 134-140.
[9] P. Xuya, L. Zhiyang, Study On Regularity Of Fumes Emitting From Asphalt, Intelligent Automation and Soft Comuption 16(5) (2010) 833-839.
[10] M. Wang, P. Li, T. Nian, Y. Mao, An overview of studies on the hazards, component analysis and suppression of fumes in asphalt and asphalt mixtures, Construction and Building Materials 289 (2021) 123185.
[11] D. Zhang, M. Chen, S. Wu, Q. Liu, J. Wan, Preparation of expanded graphite/polyethylene glycol composite phase change material for thermoregulation of asphalt binder, Construction and Building Materials 169 (2018) 513-521.
[12] P.Q. Cui, S.P. Wu, Y. Xiao, H.H. Zhang, Experimental study on the reduction of fumes emissions in asphalt by different additives, Materials Research Innovations 19(sup1) (2015) S1-158-S1-161.
[13] F. Xiao, X. Peng, S. Qian, A Study On Addictives For Fume Reduction In Asphalt Pavement Construction, Intelligent Automation & Soft Computing 16(5) (2010) 797-803.
[14] S.L. Qian, F. Wang, The Experimental Study on the Road Asphalt Fumes Inhibitors, Advanced Materials Research 413 (2012) 472-476.
[15] T. Xu, H. Wang, X. Huang, G. Li, Inhibitory action of flame retardant on the dynamic

evolution of asphalt pyrolysis volatiles, Fuel 105 (2013) 757-763.
[16] P.K. Ashish, D. Singh, S. Bohm, Evaluation of rutting, fatigue and moisture damage performance of nanoclay modified asphalt binder, Construction and Building Materials 113 (2016) 341-350.
[17] E. Iskender, Evaluation of mechanical properties of nano-clay modified asphalt mixtures, Measurement 93 (2016) 359-371.
[18] T. Ono, M. Ohta, K. Iseda, K. Sada, Counter anion dependent swelling behaviour of poly(octadecyl acrylate)-based lipophilic polyelectrolyte gels as superabsorbent polymers for organic solvents, Soft Matter 8 (2012).
[19] T. Ono, S. Shinkai, K. Sada, Discontinuous swelling behaviors of lipophilic polyelectrolyte gels in non-polar media, Soft Matter 4(4) (2008) 748-750.
[20] T. Ono, T. Sugimoto, S. Shinkai, K. Sada, Molecular Design of Superabsorbent Polymers for Organic Solvents by Crosslinked Lipophilic Polyelectrolytes, Advanced Functional Materials 18(24) (2008) 3936-3940.
[21] E.M. Ahmed, Hydrogel: Preparation, characterization, and applications: A review, Journal of advanced research 6(2) (2015) 105-21.
[22] I. Menapace, W. Yiming, E. Masad, Effects of Environmental Factors on the Chemical Composition of Asphalt Binders, Energy & fuels 33 (2019) 2614-2624.
[23] M. Han, J. Li, Y. Muhamma, D. Hou, F. Zhang, Y. Yin, S. Duan, Effect of polystyrene grafted graphene nanoplatelets on the physical and chemical properties of asphalt binder, Construction & Building Materials 174 (2018) 108-119.
[24] M. Han, J. Li, Y. Muhammad, Y. Yin, J. Yang, S. Yang, S. Duan, Studies on the secondary modification of SBS modified asphalt by the application of octadecyl amine grafted graphene nanoplatelets as modifier, Diamond and Related Materials 89 (2018) 140-150.
[25] T. Ono, T. Sugimoto, S. Shinkai, K. Sada, Lipophilic polyelectrolyte gels as super-absorbent polymers for nonpolar organic solvents, Nature Materials 6(6) (2007) 429-433.
[26] ASTM, D4124-09, Standard Test Method for Separation of Asphalt into Four Fractions, American Society of Testing Materials, 2018.
[27] MOT, T 0618-1993, Standard Test Method of Asphalt Chemical Component Analysis (Four Components Method), Ministry of Transport of the People's Republic of China, 2019.
[28] T. Nian, P. Li, Y. Mao, G. Zhang, Y. Liu, Connections between chemical composition and rheology of aged base asphalt binders during repeated freeze-thaw cycles, Construction and Building Materials 159 (2018) 338-350.
[29] Y. Liu, J. Li, C.H. Wu, Asphalt Material Aging Mechanism and Characteristics Analysis Based on Infrared Spectrum, Advanced Materials Research 652-654 (2013) 1265-1268.
[30] Y. Wei, Y. Liu, Y. Muhammad, S. Subhan, F. Meng, D. Ren, M. Han, J. Li, Study on the properties of GNPs/PS and GNPs/ODA composites incorporated SBS modified asphalt after short-term and long-term aging, Construction and Building Materials 261 (2020) 119682.
[31] A. Sreeram, Z. Leng, R. Hajj, W.L.G. Ferreira, Z. Tan, A. Bhasin, Fundamental investigation of the interaction mechanism between new and aged binders in binder blends, International Journal of Pavement Engineering 23(5) (2022) 1317-1327.
[32] A. Sreeram, Z. Leng, Y. Zhang, R.K. Padhan, Evaluation of RAP binder mobilisation and blending efficiency in bituminous mixtures: An approach using ATR-FTIR and artificial aggregate, Construction and Building Materials 179 (2018) 245-253.
[33] X. Zhou, T.B. Moghaddam, M. Chen, S. Wu, S. Adhikari, Biochar removes volatile organic compounds generated from asphalt, The Science of the total environment 745 (2020) 141096.

[34] AASHTO, T 315, Determining the Rheological Properties of Asphalt Binder Using a Dynamic Shear Rheometer (DSR), American Association of State Highway and Transportation Officials, 2022.
[35] AASHTO, M 320, Standard Specification for Performance-Graded Asphalt Binder, American Association of State Highway and Transportation Officials, 2022.
[36] AASHTO, T 350, Standard Test Method for Multiple Stress Creep and Recovery (MSCR) of Asphalt Binder Using a Dynamic Shear Rheometer, American Association of State Highway and Transportation Officials, 2019.
[37] AASHTO, T 391, Standard Method of Test for Estimating Fatigue Resistance of Asphalt Binders Using the Linear Amplitude Sweep, American Association of State Highway and Transportation Officials, 2020.
[38] K. Ganesh, E.H. El-Mossalamy, A. Satheshkumar, C. Balraj, K.P. Elango, Molecular complexes of l-phenylalanine with substituted 1,4-benzoquinones in aqueous medium: Spectral and theoretical investigations, Spectrochimica Acta Part A: Molecular and Biomolecular Spectroscopy 116 (2013) 301-310.
[39] A.G. Farzan, T. Helena, Graphene feasibility and foresight study for transport infrastructures, Chalmers Industriteknik 16 (2016) 234-246.
[40] V.F. Korolovych, V. Cherpak, D. Nepal, A. Ng, N.R. Shaikh, A. Grant, R. Xiong, T.J. Bunning, V.V. Tsukruk, Cellulose nanocrystals with different morphologies and chiral properties, Polymer 145 (2018) 334-347.
[41] E. Zahir, R. Saeed, M.A. Hameed, A. Yousuf, Study of physicochemical properties of edible oil and evaluation of frying oil quality by Fourier Transform-Infrared (FT-IR) Spectroscopy, Arabian Journal of Chemistry 10 (2017) S3870-S3876.
[42] T.R. Board, E. National Academies of Sciences, Medicine, Mixing and Compaction Temperatures of Asphalt Binders in Hot-Mix Asphalt, The National Academies Press, Washington, DC, 2010.
[43] W. Wang, Y. Zhang, W. Liu, Bioinspired fabrication of high strength hydrogels from non-covalent interactions, Progress in Polymer Science 71 (2017) 1-25.
[44] X. Zhang, Y. Xiao, Y. Long, Z. Chen, P. Cui, R. Wu, X. Chang, VOCs reduction in bitumen binder with optimally designed Ca(OH)2-incorporated zeolite, Construction and Building Materials 279 (2021) 122485.